Interaction of the Neurotransmitter, Neuropeptide Y, with Phospholipid Membranes: Infrared Spectroscopic Characterization at the Air/Water Interface†

Martina Dyck,‡ Andreas Kerth,§ Alfred Blume,§ and Mathias Lösche*,∥,⊥

University of Leipzig, Institute of Experimental Physics I, D-04103 Leipzig, Germany, Martin Luther University, Institute of Physical Chemistry, D-06108 Halle, Germany, Carnegie Mellon University, Department of Physics, Pittsburgh, Pennsylvania 15213-3890, and CNBT Consortium, NIST Center for Neutron Research, Gaithersburg, Maryland 20899-8562

Received: April 25, 2006; In Final Form: August 8, 2006

The association of neuropeptide Y (NPY) at the air/water interface and with phospholipid monolayers on water as subphase has been investigated using external infrared reflection absorption spectroscopy (IRRAS). Studies of the conformation and orientation of NPY suggest that it adopts an α-helical structure and is oriented parallel to the air/water interface in neat peptide monolayers. Both secondary structure and orientation are preserved in mixed lipid/NPY monolayers. Comparison of NPY associated with zwitterionic DPPC and with anionic DMPS suggests that electrostatic attraction plays a major role for peptide binding to the membrane surface.

1. Introduction

Membrane binding is an essential step for many ligands that target membrane-embedded receptors. As first shown quantitatively by Adam and Delbrück,[1] one important role of membranes in biology that goes beyond the obvious, i.e. the two-dimensional (2D) organization of membrane components, may concern a reduction of dimensionality for the travel of signal molecules, such as hormones and peptides, to their specific membrane receptors. In such a scenario, the signal molecule would adsorb to a membrane surface and diffuse there in a 2D rather than a 3D random walk, thereby enhancing its efficiency in finding the receptor.

Neuropeptide Y (NPY) is a 36 amino acid neurotransmitter peptide with an amidated C-terminus. It is found throughout the central and peripheral nervous system of many mammalian species, including humans,[2] and has been one of the most intensively studied peptides in pharmacological and structural research in the last years. The sequence of human NPY (hNPY) is YPSKP DNPGE DAPAE DMARY YSALR HYINL ITRQR Y−NH_2. The NOE pattern of hNPY in solution suggests the presence of an amphiphilic α-helix, which spans residues 13−36, while the N-terminal part of the peptide is disordered.[3]

In the previous paper of this issue,[4] we investigated thermodynamical aspects and the lateral organization on the optical length scale of NPY in aqueous surface layers and showed that surface monolayers (Langmuir films) are an appropriate system to investigate the association of the signal peptide with membrane surfaces. We demonstrated that the studies of such systems on pure water as a subphase (rather than physiological buffer) captures many relevant aspects of that interaction and provided circumstantial evidence that systems prepared by co-spreading of mixed lipid/peptide solutions have similar properties to systems prepared by adsorption of peptides from the subphase to preformed lipid monolayers. One major conclusion from that work was that the integrity of the α-helix is not particularly important for membrane binding, as derived from a comparison of native NPY with a derivative, Y20P−NPY, which bears a proline substitution in the center of the helical section. Thermodynamic data also suggested that peptide association with negatively charged monolayer surfaces ($DMPS^-$) was somewhat stronger than, *but not qualitatively different from*, that with zwitterionic surfaces (DPPC).

Infrared reflection absorption spectroscopy (IRRAS) provides a powerful tool to study Langmuir monolayers noninvasively with respect to molecular organization and molecular interactions.[5−7] IR has grown into a standard technique to assess lipid conformation and phase behavior and is also an important and established method for molecular characterization of proteins.[8,9] IRRAS is currently the only physical method capable of monitoring directly the secondary structure of peptides associated with Langmuir films in situ.[10] In this paper, we use IRRAS to study the orientation and secondary structure of NPY in neat peptide monolayers and in mixed lipid/NPY monolayers as well as to obtain information about structural parameters within the monolayer such as lipid acyl chain conformation and orientation. This adds molecular-level detail to the thermodynamic results reported in the previous paper[4] and will specifically show that those results underestimate the role of electrostatic interactions in the membrane association of NPY.

2. Materials and Methods

For further details, see previous paper in this issue, ref 4.

A. Materials. Human neuropeptide Y (hNPY) was a generous gift from A. G. Beck-Sickinger (Leipzig, Germany) or was purchased from AnaSpec (San Jose, CA). Dipalmitoylphosphatidylcholine (DPPC) from Sigma-Aldrich (Deisenhofen, Germany) and dimyristoylphosphatidylserine (DMPS) from Avanti Polar Lipids (Alabaster, AL) were used as supplied. Water used as the subphase for Langmuir films was filtered in a Millipore MilliQ system, yielding a residual specific resistance of greater than 18.2 MΩ cm. HPLC grade chloroform and methanol (Merck, Darmstadt, Germany) were used as spreading solvents. Surface layers were spread from lipid, peptide, or premixed lipid/peptide solutions in chloroform/methanol (3:1) on pure water.

† Part of the special issue "Charles M. Knobler Festschrift".

* Corresponding author. E-mail: quench@cmu.edu.
‡ University of Leipzig.
§ Martin Luther University.
∥ Carnegie Mellon University.
⊥ CNBT Consortium.

10.1021/jp062537q CCC: $33.50
Published on Web 10/21/2006

B. Methods. *Langmuir Film Balance.* All experiments were performed on a custom-built film balance (Riegler & Kirstein, Berlin, Germany) using ash-free filter paper as a Wilhelmy plate. The teflon film balance consists of a sample (300 × 60 × 3 mm^3) and a reference (60 × 60 × 3 mm^3) trough, linked by three tubes to ensure consistent height of both air/water interfaces.[11] Before each experiment, the trough was cleaned with Hellmanex (Fisher Scientific GmbH, Nidderau, Germany) and copiously rinsed with pure water. The subphase temperature was maintained at 20 ± 0.5 °C for all experiments. Chloroform/methanol (3:1) solutions of the lipid or lipid/peptide mixture were spread at the air/water interface. After an equilibration period of at least 15 min, the surface pressure/area isotherms ($\pi-A$ isotherms) were recorded with a compression speed of 0.03 nm^2 per (molecule × minute).

IRRAS. Infrared spectra were recorded on an Equinox 55 FTIR spectrometer equipped with an XA 511 reflection attachment (Bruker, Karlsruhe, Germany) and an external narrow band MCT detector. The IR beam is directed onto the water surface at a selectable angle of incidence, α_i, by a mirror system. A computer-controlled rotating KRS-5 polarizer is used to generate parallel (p) and perpendicularly (s) polarized light. The trough is mounted on a shuttle platform that enables switching of the beam position between the sample and the reference trough. This capability is critical to correct for water vapor absorption in the light beam.[12] To achieve this, the system is enclosed to keep the relative humidity constant.

Spectra were recorded along a $\pi-A$ isotherm by compressing the film to a desired area per molecule, followed by a wait time of 10 s. For routine measurements at a fixed angle, α_i was usually set to 40° (measured with respect to the surface normal) and spectra were recorded by co-addition of 1000 scans at a resolution of 4 cm^{-1} using Blackman−Harris four-term apodization and a zero filling factor of 2. The reflection absorption (RA) is then computed as $-\log(R/R_0)$, where R_0 and R are the reflectivities of the pure and the film-covered surface, respectively. For the determination of band center positions, typically 10 independent spectra were co-added to increase the signal-to-noise ratio.

To determine the orientation of transition dipole moments, IRRA spectra measured with p- and s-polarized light (4000 and 2000 scans, respectively) were recorded at various angles α_i between 32 and 68° at 4° intervals, omitting the region near the Brewster angle. For such measurements, the spectral resolution was set to 8 cm^{-1} using Blackman−Harris four-term apodization and a zero filling factor of 2.

Data Analysis. Peak positions and band intensities were evaluated using the OPUS software (Bruker). In several cases, a water vapor subtraction was performed using OPUS. The polarizer efficiency in the $\nu(CH_2)$ region was determined as 0.018. Spectrum simulations based on the optical theory[13,14] were performed using a Yorick (made available by Lawrence Livermore National Laboratory through ftp://ftp-icf.llnl.gov/pub/Yorick/, as accessed in August, 2006) script that implements a published formalism.[15,16]

3. Results

Neat Peptide Monolayers. *Isotherms.* NPY contains an α-helical region which extends over the region, Pro13 to Tyr36.[3] This amphiphilic helix is best defined between Asp16 and Arg33.[17] The peptide associates readily with the water surface and forms Langmuir films, due to its amphiphatic character, that withstand significant surface pressure when spread from chloroform/methanol solution.[4] At $\pi \sim 12$ mN/m, a plateau appears in the π/A curve (see inset in Figure 1), which is a characteristic feature of many amphiphatic α-helical peptides and is often interpreted as the collapse of the surface-associated layer of helices at a specific surface pressure, π_{col}.[18,19] For NPY, the surface area occupied by the peptide in the films correlates with its molecular dimensions.[4] While this area depends to some extent on the concentration of the spreading solution, the π/A curve shows characteristic features that are also observed in NPY/lipid surface films, which in turn are stable and are dominated by the thermodynamics of the lipid component. It has thus been concluded[4] that the peptide associates at the water surface (or with the hydrophobic core of a lipid membrane in contact with water) with its long axis along the interface below $\pi_{col} = 12$ mN/m; it is displaced from this interface upon compressing the film beyond π_{col} and may self-associate at higher π to shield its hydrophobic faces from water exposure.

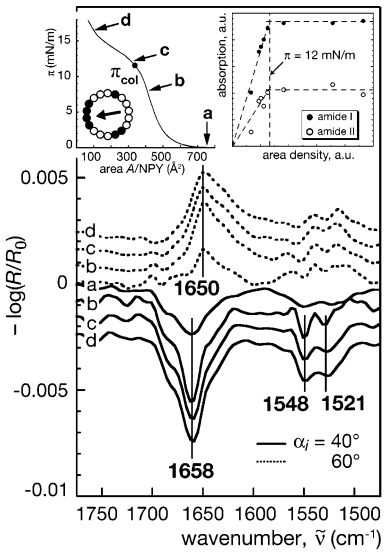

Figure 1. Amide region of IRRA spectra (p-polarization, $\alpha_i = 40°$ and 60°, $T = 20$ °C) of an NPY film on water during compression. Characters at the spectra correspond with those in the $\pi-A$ curve shown in the left inset (a: $\pi = 0$ mN/m; b: 8 mN/m; c: 12 mN/m; d: 16 mN/m). Also shown is a helical wheel representation of the NPY α-helix that indicates its pronounced amphiphatic character (black: hydrophobic residues; white: hydrophilic residues; arrow: direction of the hydrophobic moment; see also ref 4). The right inset shows the amide band intensities as a function of area density.

IRRAS. Figure 1 shows the amide region of IRRA spectra measured with p-polarized light at $\alpha_i = 40°$ and 60°, recorded during compression of an NPY surface layer. At all states of compression, the spectra contain a strong absorption band at 1658 cm^{-1}, the amide I mode, which is mainly associated with the C═O stretching mode of the peptide backbone. The position of this band is conformationally sensitive[8] and indicates that NPY incorporates an α-helical secondary motif at the air/water interface. In addition, the amide II band at 1548 cm^{-1} indicates an α-helical component. The amide I band shows a high-frequency shoulder (∼1685 cm^{-1}) that may arise from a turn or a loop in the peptide.[8] (Because the spectra are not completely compensated for water vapor bands, such features are difficult to attribute. Similarly, a small spectral contribution might be due to residual water vapor bands or might even indicate a small fraction of the peptide that incorporates a β-motif.) Since NPY incorporates 5 tyrosine residues, the band in the amide II region at ∼1520 cm^{-1} can be attributed to C−H in-plane bending and C−C stretching vibrations of tyrosine.[20] Because there is at most a very minor contribution of the amide I absorption near 1630

TABLE 1: Parameters Used in Band Simulations

system	length (Å)	width (Å)	α^a (deg)	β^a (deg)	k_{max}	n_{eo}, n_o
DPPC	19.3	5	90 (as) 90 (s)	90 (as) 0 (s)	0.6 (as) 0.3 (s)	1.41[c]
DMPS	16.7	5	90(as) 90 (s)	90 (as) 0 (s)	0.6 (as) 0.3 (s)	1.41[c]
α-helix (NPY)	27	12	36 (a I) 90 (a II)	45 (a I) 45 (a II)	1.40 (a I)[b] 0.67 (a II)[b]	1.41[c]

[a] α, β: polar angles of the transition dipole moment; as: antisymmetric; s: symmetric; a I: amide I; a II: amide II; k_{max}: starting values for the absorption coefficient of $\nu_{as}(CH_2)$ and $\nu_s(CH_2)$ bands for DPPC and DMPS; amide I and II bands of NPY, n_{eo}, n_o: extraordinary and ordinary refractive indices. [b] Buffeteau et al. 2000, ref 35. [c] Flach et al. 1997, ref 15.

cm^{-1}, it is rather unlikely that the band at 1520 cm^{-1} should be solely attributed to a β-sheet conformation.

Helix Orientation. p-Polarized IR radiation is sensitive to the transition dipole orientation with respect to the surface normal, i.e., molecular tilt, while s-polarized radiation is relatively insensitive.[15,21,22] The measurements with p-polarized light show increasing negative band intensities with α_i, up to ~50° (for an α-helix oriented along the interface). The intensity then decays and crosses zero at the Brewster angle ($\alpha_i^B \sim 55°$). As observed in Figure 1, the IRRA spectra of hNPY monolayers show negative bands at $\alpha_i = 40$ and positive bands at 60° with p-polarized light. The ratio between the amide I and II band intensities remains constant along the $\pi-A$ curve, consistent with the assumption that no change of helix orientation occurs upon compression. As the second inset in Figure 1 shows, the amide band intensities increase linearly during monolayer compression. This increase levels sharply off at π_{col}.

To interpret the spectra in terms of peptide organization more quantitatively, band simulations were performed using the parameters shown in Table 1. Figure 2 displays the simulated amide I and II bands for different tilt angles φ of the α-helix relative to the surface normal (cf. inset in Figure 2b) for p-polarized light at $\alpha_i = 40°$ and 60°. When the helix is parallel to the interface ($\varphi = 90°$), these simulations predict purely negative bands (amide I and II) at 40°, while for a helix orientation normal to the interface, a distinctive positive lobe of the amide I band is expected. Conversely, at $\alpha_i = 60°$, a strong negative lobe of the amide I band would be expected for $\varphi = 0°$, whereas for $\varphi = 90°$, the band should be purely positive in accordance with the experimental results. A comparison between experiment and simulation leads to the conclusion that the α-helix of NPY is nearly parallel to the air/water interface. The red-shift of the amide I band by 5 cm^{-1} for $\alpha_i > \alpha_i^B$ is also reproduced in the band simulations.

Lipid and Lipid/Peptide Monolayers. *Isotherms.* The association of NPY with DPPC and with $DMPS^-$, as assessed from surface pressure isotherms, has been discussed in detail in the preceding paper.[4] Both lipid monolayers show significant area expansion upon NPY incorporation and additional plateaus at higher surface pressures, π_{col}. This second transition indicates the displacement of peptide into the subphase. The peptide-induced expansion is more pronounced with $DMPS^-$, as is the shift in π_{col} (from ~14 mN/m for DPPC/NPY to >22 mN/m for $DMPS^-$/NPY), indicating significantly stronger electrostatic interactions between the anionic lipid and the peptide.

IRRAS. In this work, the interaction of the peptide with monolayers of these lipids was further studied by measuring the IRRA spectra at $\pi \sim 12$ mN/m, where the peptide is incorporated into the lipid monolayer, and at 40 mN/m, where the peptide is squeezed out. These spectra are presented in three sections: the first section displays the spectral region between 3750 and 2500 cm^{-1} (Figure 5), the second zooms into the carbonyl and amide band region (Figure 6), and the third section shows the spectral region of the lipid headgroup bands between 1300 and 950 cm^{-1} (Figure 8).

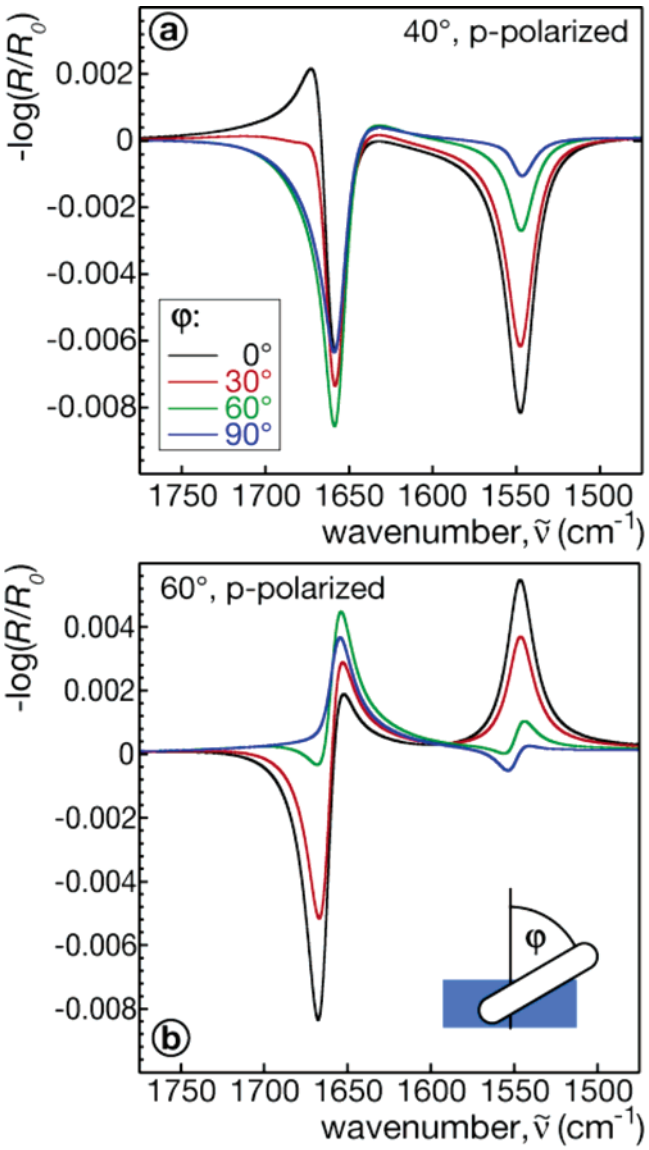

Figure 2. Simulation of the amide I and II bands (p-polarization, $\alpha_i = 40$ and 60°) of NPY for different tilt angles φ of the α-helix from the surface normal (inset in panel b).

Band Analysis: Region between 3750 and 2500 cm^{-1}. Figures 3−5 describe the spectral characteristics observed in the region between 3750 and 2500 cm^{-1}. The bands at 2920 and 2850 cm^{-1} are the well-characterized $\nu_{as}(CH_2)$ and $\nu_s(CH_2)$ stretching modes of the lipid chains (Figure 5). A shoulder at ~2958 cm^{-1} originates from the $\nu_{as}(CH_3)$ stretching vibration. At $\pi = 12$ mN/m, the $\nu(CH_2)$ band intensities are greatly reduced by NPY; on the other hand, they are identical with and without peptide at 40 mN/m. The intensity reduction observed at a pressure of 12 mN/m is most likely caused by a decrease in surface concentration of the lipid. This is well in line with the hypothesis, derived from the analysis of the isotherms, that the peptide is tightly associated with the lipid below π_{col} and is in fact intercalating into the lipid monolayer, thus replacing lipids, but is expelled from the surface layer upon compression beyond π_{col}. At first sight, at both low and high pressure, the spectral

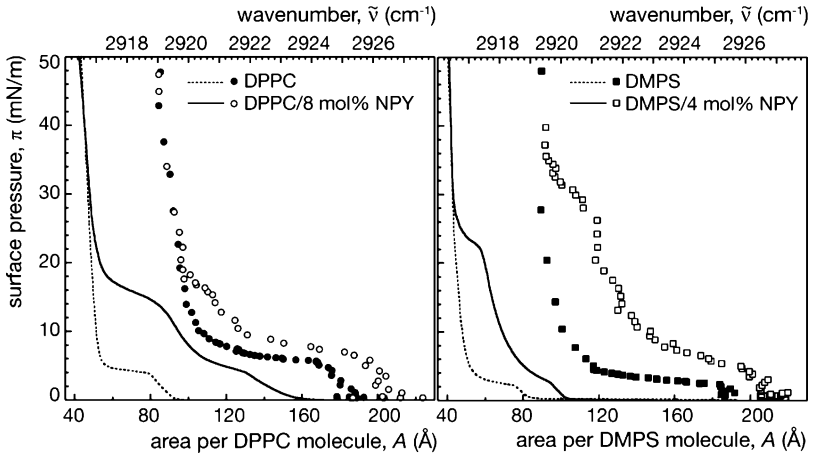

Figure 3. $\pi-A$ isotherms of DPPC (left) and DMPS (right) monolayers on water ($T = 20$ °C) without (dashed lines) and with (solid line) NPY. Discrete plot symbols show $\nu_{as}(CH_2)$ band center wavenumbers at the respective surface pressures.

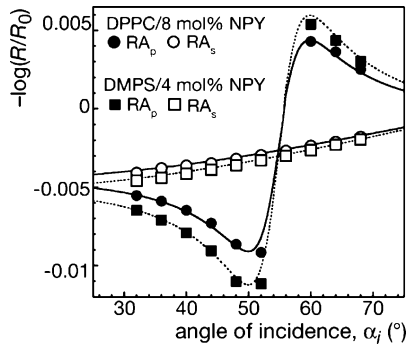

Figure 4. Comparison of simulated (solid and dashed lines) and measured peak intensities (RA_p, RA_s: p- and s-polarized reflection−absorption, respectively) of the $\nu_{as}(CH_2)$ stretching vibration band of mixed DPPC/NPY and DMPS/NPY films as a function of angle of incidence.

properties appear to be independent of the nature of the host lipid (Figure 5), but in the following, we will examine this preliminary conclusion more quantitatively.

It is well-established that the $\nu(CH_2)$ modes are highly sensitive to chain conformation.[23,24] Positions at ~2925 cm^{-1} for the $\nu_{as}(CH_2)$ stretching vibration are indicative of a substantial disorder of the acyl chains, i.e., a high concentration of gauche conformations. Figure 3 shows the correlation between the $\pi-A$ isotherms and the center positions of the lipid $\nu_{as}(CH_2)$ modes with and without NPY. It is quite obvious that vibrational frequencies and area values are closely related to each other because they show the same dependence on π. For the pure lipid monolayers, the band center wavenumbers of the $\nu_{as}(CH_2)$ mode decrease rapidly as π increases to ~10 mN/m for DPPC and ~5 mN/m for DMPS. At these points, with molecular areas $A < 60$ $Å^2$ per lipid, the phase transitions are complete, as indicated by band center values, $\nu_{as}(CH_2) < 2920$ cm^{-1}.[25] Just as observed in the corresponding isotherms, NPY induces substantial lipid chain disorder in the acyl chains. In particular, in DMPS monolayers, $\nu_{as}(CH_2)$ bands are significantly blue-shifted from the positions they attain in the pure lipid monolayer at comparable surface pressures. Starting at π_{col}, a further decrease in the band positions occurs upon compression, and the two $\tilde{\nu}$ vs π dependencies collapse on those of the respective pure monolayers. At higher π, the $\nu_{as}(CH_2)$ band frequencies are the same as for the pure lipid films.

Acyl chain tilt angles θ were determined, as shown in Figure 4, by measuring $\nu(CH_2)$ band intensities with s- and p-polarized light as a function of α_i and using an established procedure[15] for the evaluation with model parameters shown in Table 1. As the theory does not apply to disordered lipid phases, these measurements were only performed at $\pi = 40$ mN/m. The peaks were observed to be negative for all measurements of α_i with s-polarized light, while with p-polarized light, the peak intensities cross zero at α_i^B. Results for DPPC and DMPS, respectively, were quite similar irrespective of the presence of NPY in the system, consistent with other data, which indicated that the peptide is expelled from the membrane surface at high pressure. Tilt angles of ~25° and ~28° were obtained for DPPC without and with peptide, respectively. DMPS chains of were untilted both with or without NPY. The results are in good agreement with GIXD measurements,[26] see Table 2.

An entirely different approach to estimate the overall thickness of the organic surface layer was derived from an analysis of the broad water absorption band in the same spectral region. Selected spectra between 3750 and 2500 cm^{-1} are shown in Figure 5. The broad, strong absorption at ~3600 cm^{-1} arises from the $\nu(O-H)$ stretching vibration of water. It has been recently shown that its intensity correlates with the thickness of the anisotropic film deposited at the air/water interface, increasing as the film thickness increases.[27] This band, as well as the water association band at ~2150 cm^{-1} and the $\delta(H_2O)$ bending mode of water at ~1650 cm^{-1}, appear due to a difference of the refractive indices of the optically anisotropic organic layer and the water subphase. The intensity of these bands depends on the extraordinary and ordinary refractive indices, as well as the thickness and orientation of the optical axis of the anisotropic surface layer. Hence, qualitative information (and, if other system properties remain constant, *quantitative* information) on the film thickness and the behavior of the acyl chains at the air/water interface in the absence and presence of NPY can be deduced.

At a pressure of 12 mN/m, a decrease of the water $\nu(O-H)$ intensity upon addition of NPY is observed in the spectra for both lipid films (*cf.* dotted and solid lines in Figure 5). This decrease is, however, mainly due to a decrease in lateral lipid density within the observation spot and can be corrected for from a comparison of the $\nu(CH_2)$ band intensities in the same spectra. Owing to the dependence of the $\nu(CH_2)$ center frequencies on conformation, this adjustment can even be performed for the same physical state as in the mixed surface layer. To adjust the intensities of the bands at low surface pressure, spectra of the pure lipid were measured at surface pressures, where the $\nu(CH_2)$ band frequencies coincided with those observed in the mixed peptide/lipid spectra. They were subsequently scaled to

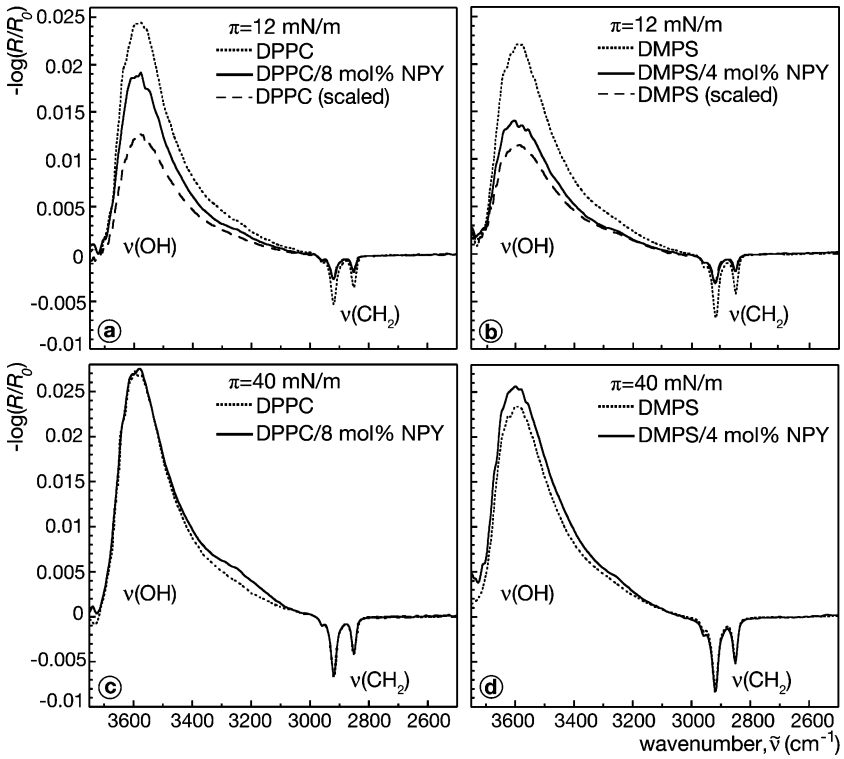

Figure 5. IRRA spectra (p-polarization, $\alpha_i = 40°$, $T = 20$ °C) of DPPC and DPPC/8 mol % NPY (a/c) and DMPS and DMPS/4 mol % NPY (b/d) monolayers on water at $\pi = 12$ and 40 mN/m, respectively. In addition, panels a and b contain neat lipid spectra that are scaled to the same lipid density as in the mixed film (cf. text).

TABLE 2: k_{max} Values and Tilt Angles of Lipid Chains Obtained from IRRAS Measurements in Comparison with Tilt Angles Determined by GIXD Measurements at $\pi = 40$ mN/m

system	k_{max}	θ (deg) IRRAS	θ (deg) GIXD[a]
DPPC	0.67 (as) 0.42 (s)	25 ± 3	30
DPPC/8 mol % NPY	0.70 (as) 0.43 (s)	28 ± 3	30
DMPS	0.71 (as) 0.43 (s)	untilted	untilted
DMPS/4 mol % NPY	0.73 (as) 0.45 (s)	untilted	untilted

[a] Reference 26.

match the $\nu(CH_2)$ intensities of the mixed films. The resulting correction implies that the equivalent lipid area densities were only ~60% for DPPC/8 mol % NPY and 70% for DMPS/4 mol % NPY of those in the neat lipid monolayers at $\pi = 12$ mN/m. The adjusted water ν(O−H) intensities (dashed lines in Figure 5a, b), and thus the overall organic film thicknesses on the water surface, are then larger for the NPY/lipid films than for the films without peptide, and the difference is larger for DPPC than for DMPS, suggesting that the effect depends on peptide concentration in the monolayer. On the other hand, at $\pi = 40$ mN/m, $\nu(CH_2)$ intensities are identical with and without peptide, so that no correction of the band intensities is necessary. Similarly, the water ν(O−H) intensities for the DPPC and the DPPC/NPY monolayers are identical: lipid conformation is no longer affected by the peptide. The DMPS/NPY monolayer at high π is somewhat in between. While the intensity of the ν(O−H) band is substantially higher than for the pure DMPS monolayer at the same pressure, the difference is significantly smaller than that at low π.

Carbonyl and Amide Region. The spectral region from 1800 to 1500 cm^{-1} that contains the lipid carbonyl band, ν(C═O), is displayed in Figure 6. This band is located between 1725 and 1740 cm^{-1} and is overlapped in the pure lipid spectra by a maximum in the baseline at ~1650 cm^{-1}, caused by the H_2O bending mode of water. NPY association with monolayers affects the spectral features in this region by reducing the ν(C═O) intensity and by superimposing the peptide amide bands on the spectra, most notably at $\pi = 12$ mN/m. At this surface pressure, the amide I band at 1658 cm^{-1} is clearly visible, and the amide II band appears at 1548 cm^{-1}. As with pure peptide films, these band absorption frequencies indicate a structure dominated by the α-helix motif. In fact, the amide band positions are the same as in the pure peptide monolayer. For the DPPC/NPY monolayer at $\pi = 40$ mN/m, the amide bands have completely disappeared and the spectrum matches with that of the neat DPPC monolayer. For the DMPS/NPY monolayer, on the other hand, the amide bands are still visible at high surface pressures.

The phospholipid ν(C═O) modes are sensitive to hydrogen bonding.[28] Band centers at $\tilde{\nu} = 1740-1742$ cm^{-1} are associated with dehydrated (i.e., non-hydrogen-bonded) C═O groups, while values between 1723 and 1728 cm^{-1} indicate hydrogen bonding to the carbonyls. Band frequencies determined in spectra such as the ones in Figure 6 as a function of π are plotted in Figure 7. At all pressures, the band positions are located between 1733 and 1736 cm^{-1} for neat DPPC and are not significantly influenced by NPY. For DMPS, the carbonyl band is observed at $\tilde{\nu} \sim 1739$ cm^{-1}, indicating dehydrated carbonyls, and NPY has a dramatic influence on its position. The band is shifted by $\Delta\tilde{\nu} \sim 11$ cm^{-1} to lower wavenumbers at $\pi = 12$ mN/m. Such large shifts indicate strong interactions between the lipid carbonyl groups and functional groups of the peptide. The wavenumber of the band position rises with increasing surface pressure and reaches almost the value of the pure DMPS at $\pi = 40$ mN/m.

Peptide Orientation in Lipid Monolayers. Panels e and f of Figure 6 show the carbonyl and amide regions of the spectra of

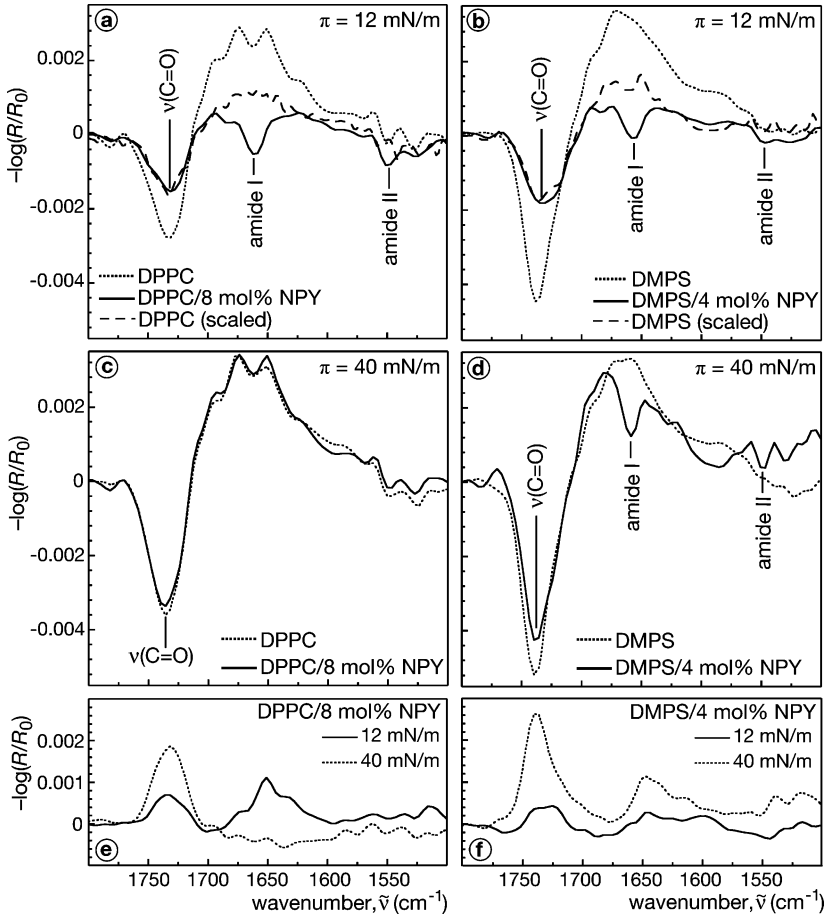

Figure 6. IRRA spectra of the amide and lipid carbonyl region for DPPC and DPPC/8 mol % NPY (a/c) and for DMPS and DMPS/4 mol % NPY (b/d) monolayers on water at $\pi = 12$ and 40 mN/m, respectively, all at $\alpha_i = 40°$. In addition, panels a and b contain neat lipid spectra that are scaled to the same lipid density as in the mixed films (cf. text). Panels e and f show lipid/NPY spectra at $\alpha_i = 60°$ for comparison.

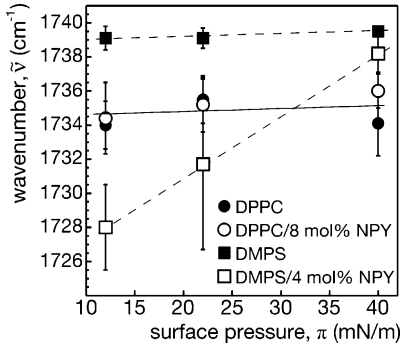

Figure 7. Surface pressure dependence of the ν(C═O) band center frequencies of DPPC (circles) and DMPS (squares) without (filled symbols) and with (open symbols) NPY, respectively. The data were derived as an average from 10 independently measured spectra such as the ones shown in Figure 6. Lines are guides for the eyes.

lipid/NPY monolayers at $\alpha_i = 60°$. All major bands are positive. As already observed for pure NPY monolayers, the positive amide bands of NPY observed in DPPC films at 12 mN/m and in DMPS films at both pressures indicate that the α-helices are aligned parallel to the air/water interface. The absence of amide band intensity in DPPC/NPY monolayers above $\pi_{col} \sim 15$ mN/m suggests that NPY is quantitatively replaced from the surface. However, as observed upon monitoring peptide reinsertion in the isotherm,[4] an expansion of the lipid film leads to a reinsertion of NPY into the monolayer, and the amide band reappears in the IRRA spectra after extended relaxation at $\pi \sim 0$. In the case of the DMPS/NPY monolayer, the amide bands of NPY are still visible at 40 mN/m. Since the amide bands are still positive at an angle of incidence of 60°, we conclude that the α-helix does not change its orientation but is still roughly parallel to the interface, even while the peptide is squeezed out of the monolayer.

Region between 1300 and 950 cm^{-1}. Figure 8a compares spectra of the fingerprint region of the lipid headgroup vibrations in DPPC and DMPS at $\pi = 40$ mN/m. Five bands are observed for DPPC (dotted line), and are assigned to the antisymmetric PO_2^- stretching mode $\nu_{as}(PO_2^-)$ at ∼1226 cm^{-1}, ν(CO−O) at ∼1164 cm^{-1}, and $\nu_s(PO_2^-)$ at 1088 cm^{-1}.[29] The shoulder near 1060 cm^{-1} is due to the ν(C−O−P−O−C) mode. The antisymmetric ν_{as}(C−N$^+$−C) stretching mode of the choline group is observed at 973 cm^{-1}. IRRA spectra of DMPS (solid line in Figure 8a) reveal a red-shift of $\nu_{as}(PO_2^-)$ to 1220 cm^{-1}, while ν(CO−O) is also near 1164 cm^{-1}. In comparison to DPPC, the $\nu_s(PO_2^-)$ mode between 1089 and 1101 cm^{-1} of DMPS is less intense, followed by a strong band of the ν(C−O−P−O−C) mode.[29]

The most characteristic vibrational bands are those arising from the phosphate group. These bands depend strongly on the hydration state of the lipid headgroup[30] and are sensitive to hydrogen bonding to the phosphate. Consequently, these bands are also the ones most affected by NPY interaction with the monolayer surface. Parts b and c of Figure 8 show the influence of NPY (4 mol %) on DMPS at $\pi = 12$ and 40 mN/m, respectively. At both surface pressures, $\nu_{as}(PO_2^-)$ is blue-shifted by a few wavenumbers. In contrast, the peptide influence on the lipid headgroup fingerprint region in DPPC is marginal. In fact, the spectra of the systems without and with peptide at $\pi = 40$ mN/m are virtually indistinguishable (data not shown).

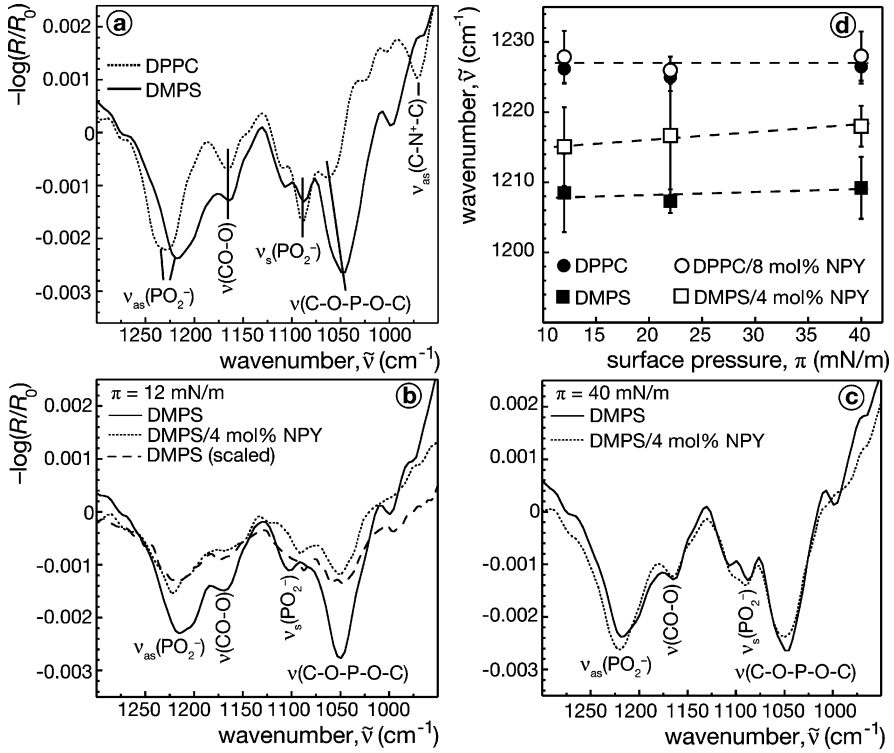

Figure 8. IRRA spectra of the lipid headgroup fingerprint region (p-polarization, $\alpha_i = 40°$, $T = 20$ °C) of neat lipid monolayers ($\pi = 40$ mN/m, panel a) and of DMPS without and with NPY ($\pi = 12$ mN/m and 40 mN/m, panels b, c). Panel (d) displays the $\nu_{as}(PO_2^-)$ band center frequency as a function of π. The data in (d) were derived as an average from 10 independently measured spectra such as the ones shown in (a−c).

Figure 8d shows a plot of the $\nu_{as}(PO_2^-)$ band positions against π. No significant changes are observed for DPPC. Its $\nu_{as}(PO_2^-)$ mode appears at ∼1226 cm^{-1}, in good agreement with other values reported for hydrated phosphocholines.[31] $\nu_{as}(PO_2^-)$ in DMPS is observed between 1216 and 1208 cm^{-1} in the presence and in absence of NPY, respectively. A blue-shift to lower wavenumbers has been reported for DMPE itself and was explained with strong inter- and/or intramolecular hydrogen bonding between the NH_3^+ and PO_2^-.[32] Formation of intramolecular hydrogen bonds in phosphatidylserines has also been reported to occur in molecular dynamics simulations of bilayers.[33] The shift of the antisymmetric phosphate stretching mode from 1208 to 1216 cm^{-1} indicates additional interactions between the PO_2^- group and functional groups of the peptide. Thus, NPY appears to weaken the strong intramolecular hydrogen bonding within films of pure DMPS.

4. Discussion

The binding of a ligand to a membrane reduces the dimensionality of its diffusion pathway and increases thus the efficiency of receptor binding in systems with sizes typical of biological cells.[1] The surface thermodynamics of NPY shows that the peptide interacts strongly with lipid monolayers and suggested that this interaction is similar with zwitterionic and with anionic lipids.[4] As we look into the molecular details with IRRAS, however, it becomes clear in this work that the peptide interacts substantially stronger with DMPS$^-$ than with DPPC. Among other implications, this may provide for a mechanism which facilitates receptor binding once the transmitter encounters the receptor in the trajectory of its 2D random walk along the membrane surface.[4] The IRRAS results presented here help to characterize the underlying interactions in molecular detail and to provide more definite answers regarding the association of the peptide with the biomimetic model surfaces.

The dichroism of the amide modes, Figure 4, indicates that the NPY α-helix is oriented coplanar with the water surface. The data in Figure 6 indicate that it is likely in a similar orientation when associated with lipid monolayers (however, it remains undetected in the case of NPY/DPPC at high surface pressure, see below). These results match those from NMR investigations of the peptide in micellar solutions[17] and have also been inferred from the surface isotherms.[4] More generally, in studies of peptide association with membrane surfaces, it is often observed that such a coplanar arrangement is the preferred arrangement of α-helical peptides.[34]

The small compression−expansion−recompression hystereses in isotherms[4] suggests that NPY stays associated with the monolayer surface above π_{col}. The pronounced differences in the water ν(O−H) modes, Figure 5, show significant differences for DPPC and DMPS$^-$, however. At low π (Figure 5a, b), the strong increase in the adjusted ν(O−H) intensity indicates that the overall surface layer thickness is substantially increased if NPY is present. Conversely at high π, the spectra with and without the peptide are virtually indistinguishable in the case of DPPC (Figure 5c): the peptide is spectroscopically invisible. With DMPS at high π, on the other hand, the ν(O−H) intensity is increased by the peptide (Figure 5d). Thus NPY exerts a quantifiable influence in the IRRAS experiment. Similar conclusions are drawn from the results on the amide vibrations (Figure 6): the peptide is still observed if expelled from the DMPS monolayer, whereas it remains invisible in the DPPC system. These differences in interaction between NPY and DPPC or DMPS are surprising given the qualitative similarity of the isotherm results. They imply that the peptide association with charged and dipolar membrane surfaces is much more distinctive than the isotherms appear to suggest.

Similar differences in the association of NPY with the two lipid species are observed in the headgroup fingerprint vibrations (Figure 8) and, most notably, ν(C═O), cf. Figures 6 and 7. Neither of these spectral regions show differences between the NPY/DPPC system and the pure DPPC monolayer at high π. Even at low π, the band wavenumbers of ν(C═O) coincide for

DPPC with and without NPY, indicating that the lipid backbone does not interact with the peptide. Distinct from from DPPC, DMPS with NPY at low π shows a large red-shift in its ν(C═O) band center frequency from the position observed in pure DMPS that disappears progressively as the surface layer is compressed (Figure 7). At 40 mN/m, the ν(C═O) bands of DMPS with and without NPY are again indistinguishable. This suggests that the peptide affects the carbonyl's hydrogen bonding pattern strongly at low π, either by direct hydrogen bonding or by significantly hydrating the lipid backbone upon insertion into the DMPS headgroup. This disturbance fades when the peptide is displaced from the monolayer interface. Finally, vibrations in the fingerprint region between 1250 and 900 cm^{-1} corroborate the very weak interaction of the peptide with DPPC (at low π, the spectral differences are again rather due to area density differences of the lipid than indicative of differences in the molecular interactions). In constrast, substantial shifts of the center of the $\nu(PO_2^-)$ band suggest interference of the peptide with the hydrogen bonding pattern of the PS^- headgroup and provide more evidence for direct interaction between the peptide and the lipid, in particular at low π.

5. Conclusions

In this work, the association of NPY with membrane surfaces was investigated on the molecular level using the IRRAS technique. We studied the conformation and orientation of the peptide at the air/water interface and its interaction with lipid monolayers. Consistent with studies of the structure and dynamics of NPY in solution and of micelle-bound NPY,[3,17] the peptide adopts a conformation that is dominated by the α-helical motif at lipid monolayers, both charged and zwitterionic, below the peptide collapse pressure π_{col}, identical to its secondary structure in neat peptide layers at aqueous surfaces. The axes of the helices are preferentially aligned with the interface.

Substantial differences were documented in the strength and the mode of interaction of the peptide as a function of charge on the lipid headgroup. While the interaction is marginal with the zwitterionic lecithin headgroup with which it appears loosely associated at low π and from which it is entirely dissociated above π_{col}, NPY interaction with the anionic phosphatidylserine is substantial, even above π_{col}. In fact, IRRAS shows a profound impact of the peptide on the hydrogen bonding to the lipid carbonyls and the phosphate in DMPS at low π. While its influence on the carbonyls vanishes upon compression above π_{col}, it is independent of surface pressure for the phosphate group, consistent with the finding that the peptide remains associated with the interface even after exclusion from the monolayer.

We conclude that the peptide interacts strongly with anionic lipids at membrane surfaces, whereas its interaction with zwitterionic lipids is marginal, despite its pronounced hydrophobic moment. For physiological situations, i.e. the interaction and diffusion dynamics of the signal peptide at cell membranes, this implies that NPY would likely bind to anionic membrane surfaces, even under physiological salt conditions, while it would not likely associate with pronouncedly zwitterionic membrane surfaces. In mixed membranes with substantial anionic components, the peptide might bind and preferentially recruit anionic lipids around its footprint on the membrane surface. Such scenarios suggest that peptide association with membrane surfaces is controlled by the molecular composition of the target membrane and that differences of composition within the membrane area can trigger binding or unbinding of the signal peptide in response, for example, to the presence of the receptor.

Acknowledgment. We thank A. G. Beck-Sickinger for peptide material and the Johns Hopkins University, Thomas C. Jenkins Department of Biophysics, where some of the reported work was performed, for its hospitality. This work was supported by the NSF (grant no. 0555201), the Volkswagen Foundation (I/77709), the National Institutes of Health (1RO1 RR14812), and The Regents of the University of California.

References and Notes

(1) Adam, G.; Delbrück, M. Reduction of Dimensionality in Biological Diffusion Processes. In *Structural Chemistry and Molecular Biology*; Rich, A., Davidson, N., Eds.; W. H. Freeman: New York, 1968; p 198.

(2) Allen, J. M.; Bloom, S. R. *Neurochem. Int.* **1986**, *8*, 1.

(3) Monks, S. A.; Karagianis, G.; Howlett, G. J.; Norton, R. S. *J. Biomol. NMR* **1996**, *8*, 379.

(4) Dyck, M.; Lösche, M. *J. Phys. Chem. B* **2006**, *110*, 22142.

(5) Dluhy, R. A.; Cornell, D. G. *J. Phys. Chem.* **1985**, *89*, 3195.

(6) Dluhy, R. A. *J. Phys. Chem.* **1986**, *90*, 1373.

(7) Dluhy, R. A.; Mitchell, M. L.; Pettenski, T.; Beers, J. *Appl. Spectrosc.* **1988**, *42*, 1289.

(8) Goormaghtigh, E.; Cabiaux, V.; Ruysschaert, J.-M. Determination of Soluble and Membrane Protein Structure by Fourier Transform Infrared Spectroscopy. In *Physicochemical Methods in the Study of Biomembranes*; Hilderson, H. J., Ralston, G. B., Eds.; Plenum Press: New York, 1994; p 405.

(9) Jackson, M.; Mantsch, H. H. *Crit. Rev. Biochem. Mol. Biol.* **1995**, *30*, 95.

(10) Cai, P.; Flach, C. R.; Mendelsohn, R. *Biochemistry* **2003**, *42*, 9446.

(11) Kerth, A.; Erbe, A.; Dathe, M.; Blume, A. *Biophys. J.* **2004**, *86*, 3750.

(12) Flach, C. R.; Brauner, J. W.; Taylor, J. W.; Baldwin, R. C.; Mendelsohn, R. *Biophys. J.* **1994**, *67*, 402.

(13) Kuzmin, V. L.; Mikhailov, A. V. *Opt. Spectrosk. (USSR)* **1981**, *51*, 383.

(14) Kuzmin, V. L.; Romanov, V. P.; Mikhailov, A. V. *Opt. Spectrosk. (USSR)* **1992**, *73*, 1.

(15) Flach, C. R.; Gericke, A.; Mendelsohn, R. *J. Phys. Chem. B* **1997**, *101*, 58.

(16) Mendelsohn, R.; Brauner, J. W.; Gericke, A. *Annu. Rev. Phys. Chem.* **1995**, *46*, 305.

(17) Bader, R.; Bettio, A.; Beck-Sickinger, A. G.; Zerbe, O. *J. Mol. Biol.* **2001**, *305*, 307.

(18) Birdi, K. *Lipid and Biopolymer Monolayers at Liquid Interfaces*; Plenum Press: New York, 1989.

(19) Maget-Dana, R. *Biochim. Biophys. Acta* **1999**, *1462*, 109.

(20) Barth, A. *Prog. Biophys. Mol. Biol.* **2000**, *74*, 141.

(21) Flach, C. R.; Xu, Z.; Bi, X.; Brauner, J. W.; Mendelson, R. *Appl. Spectrosc.* **2001**, *55*, 1060.

(22) Gericke, A.; Flach, C. R.; Mendelsohn, R. *Biophys. J.* **1997**, *73*, 492.

(23) Hunt, R. D.; Mitchell, M. L.; Dluhy, R. A. *J. Mol. Struct.* **1989**, *214*, 93.

(24) Mitchell, R. C.; Haris, P. I.; Fallowfield, C.; Keeling, D. J.; Chapman, D. *Biochim. Biophys. Acta* **1988**, *941*, 31.

(25) Snyder, R. G.; Maroncelli, M.; Strauss, H. L.; Hallmark, V. M. *J. Phys. Chem.* **1986**, *90*, 5623.

(26) Dyck, M. Lipid Headgroup Organization and Interaction of Neuropeptide Y with Phospholipid Membranes. Ph.D. Thesis, Leipzig University, 2006.

(27) Hussain, H.; Kerth, A.; Blume, A.; Kressler, J. *J. Phys. Chem. B* **2004**, *108*, 9962.

(28) Blume, A.; Hübner, W.; Messner, G. *Biochemistry* **1988**, *27*, 8239.

(29) Arrondo, J. L. R.; Goñi, F. M. *Chem. Phys. Lipids* **1998**, *96*, 53.

(30) Fringeli, U. P.; Günthard, H. H. Infrared Membrane Spectroscopy. In *Molecular Biology, Biochemistry and Biophysics*; Grell, E., Ed.; Springer: New York, 1981; p 270.

(31) Goñi, F. M.; Arrondo, J. L. R. *Faraday Discuss. Chem. Soc.* **1986**, *81*, 117.

(32) Hübner, W.; Blume, A. *Chem. Phys. Lipids* **1998**, *96*, 99.

(33) Pandit, S. A.; Berkowitz, M. L. *Biophys. J.* **2002**, *82*, 1818.

(34) Hristova, K.; Dempsey, C. E.; White, S. H. *Biophys. J.* **2001**, *80*, 801.

(35) Buffeteau, T.; Calvez, E. L.; Castano, S.; Desbat, B.; Blaudez, D.; Dufourcq, J. *J. Phys. Chem. B* **2000**, *104*, 4537.